Earth Planets Space, **60**, 973–979, 2008

Summer-time nocturnal wave characteristics in mesospheric OH and O_2 airglow emissions

A. Guharay[1], A. Taori[2], and M. Taylor[3]

[1]*Aryabhatta Research Institute of observational sciencES (ARIES), Nainital, India*
[2]*National Atmospheric Research Laboratory (NARL), Gadanki, India*
[3]*CASS, Department of Physics, Utah State University, USA*

(Received February 14, 2008; Revised July 15, 2008; Accepted July 18, 2008; Online published October 15, 2008)

The mesospheric temperature mapper (MTM) measurements on mesospheric OH (6, 2) and O_2 (0, 1) band emissions from Maui, Hawaii during July, 2002 show significant day-to-day variability. The nocturnal variability reveals prominent wave signatures with a periodicity ranging from 6 to 13 h. For better characterization of the nocturnal wave in the data, a Krassovsky's η ($\sim|\eta|e^{i\varphi}$) analysis was carried out. Deduced Krassovsky parameters show significant variability, with ranges of $|\eta| \sim 1.7$–3.9 for the OH data and $\sim$4.3–13 for the O_2 data. The phase values of Krassovsky parameters exhibit larger variability, with variations from approximately -91° to $+23^\circ$ for the OH data and -45° to -10° for the O_2 data. Comparison of these values with existing observations and models show large deviations from model values and relatively better agreements with the observed values reported by other investigators. The deduced vertical wavelength from $|\eta|$ and φ indicates that our data is mostly dominated by upward propagating waves with occasional high values $\geq$100 km, implying possible evanescent waves.
Key words: Mesosphere, nightglow, wave and tides, chemistry.

1. Introduction

Gravity waves and tides play a very important role in carrying energy and momentum from the lower atmosphere to the upper atmosphere. Their interaction with mean winds and other wave modes while passing through the middle atmosphere results in their energy and momentum being dissipated into the ambient medium and, consequently, their having a dominant role on the middle atmospheric wind and temperature field variability (Murthy, 1998). The first theoretical study of gravity wave, tides, and their effects on middle atmospheric dynamics was carried out by Hines (1960), and this study has been the focus of attention for the atmospheric science community (Fritts and Alexander, 2003). For investigations on gravity wave and tides, airglow monitoring has also been a popular tool together with radar (e.g., Vincent and Lesicar, 1991; Pancheva *et al*., 2006) and lidar (e.g., Gardner and Taylor, 1998). There have been several reports that utilize airglow monitoring to decipher the planetary waves (e.g., Takahashi *et al*., 2002), tidal features (e.g., Taori *et al*., 2005), and shorter period gravity wave activities at mesospheric altitudes (Takahashi *et al*., 1999; Taori and Taylor, 2006; Taori *et al*., 2007; Suzuki *et al*., 2007).

When a propagating wave (gravity wave) in the atmosphere passes through an airglow layer, it creates perturbations in density as well as in temperature and, therefore, such waves can be characterized based on these induced adiabatic perturbations in the intensity and temperatures of the airglow emission. It was Krassovsky (1972) who introduced a quantity η (for hydroxyl emission) to characterize the wave-induced perturbations as a ratio of normalized intensity perturbations to the associated normalized temperature perturbations. This quantity was initially defined as a real quantity, but subsequent model studies have redefined it as a complex quantity, given as $\eta = |\eta|e^{i\varphi}$. The magnitude of η is defined as

$$|\eta| = \frac{(\Delta I/\langle I\rangle)}{(\Delta T/\langle T\rangle)} \tag{1}$$

where ΔI and ΔT are the perturbation amplitude of the observed wave in the intensity and temperature data, respectively, and $\langle I\rangle$ and $\langle T\rangle$ are the time-averaged band intensity and rotational temperature, respectively. The phase part of the Krassovsky parameter is defined as

$$\Phi = \Phi_I - \Phi_T \tag{2}$$

where Φ_I and Φ_T are the phases of the observed wave in terms of intensity and temperatures, respectively. If the intensity leads the temperature, then Φ will be positive, and if the temperature leads the intensity, then Φ will be negative.

The vertical wavelength (λ_z) can also be estimated using the calculated η and Φ values as follows (Tarasick and Hines, 1990).

$$\lambda_z = \frac{2\pi\gamma H}{(\gamma-1)|\eta|\sin(\Phi)} \tag{3}$$

where $\gamma = C_p/C_v = 1.4$ is the ratio of specific heats, and $H = 6$ km is the scale height. This formula is valid for

the zenith observation and for plane waves and not valid for the evanescent waves. In this study, we have deduced the Krassovsky parameters and vertical wavelengths for the mesospheric OH and O_2 airglow emission data from Maui (20.8°N, 156.2°W), Hawaii during the summer months of 2002, when the mesospheric airglow data exhibited a larger population of principal wave with an approximately 8-h periodicity (Taori *et al.*, 2005).

2. Instrumentation and Observation

The mesospheric temperature mapper (MTM), developed at Utah State University, has been utilized for the present study. The MTM measures mesospheric OH (6, 2) and O_2 (0, 1) band emissions, and line intensity, and temperature are deduced with an accuracy of more than approximately 0.5% for intensity and temperature within 3 min. It has a large format 1024×1024-pixel cooled CCD array coupled to a 90° circular field of view telecentric lens system. The MTM uses very low bandwidth ($\Delta\lambda \sim 1.2$ nm) interference filters at five different center wavelengths (840, 846.5 nm for the OH (6, 2) band; 866, 868 nm for the O_2 (0, 1) band; 857 nm for the background emissions) in a sequential manner and an exposure time of 60 s for each filter, resulting in a cadence of 5.5 min. The CCD data are again binned into 8×8 on the chip to form 128×128 super-pixel image with a resultant zenithal foot print of 0.9×0.9 km per super-pixel for optimizing the temperature determination. The detailed information on the MTM could be found elsewhere (e.g., Taori *et al.*, 2005).

The MTM has been operating since November 2001 at Maui (20.8°N, 156.2°W), Hawaii as a part of the Maui-MALT program, which is jointly sponsored by U.S. Air Force Office of Scientific Research (AFOSR) and National Science Foundation (NSF). The observation period was the month July, 2002, when a large cluster of clear nights persisted for more than 5 h, enabling good estimates for night-to-night variability and long-period wave characterization during the summer months.

3. Results and Discussion

As part of Maui-MALT campaign, most of the July 2002 data has already been reported by Taori *et al.* (2005), who elaborated on the presence of a terdiurnal wave in the mesospheric temperature data together with its relation to wind fields. However, a detailed study on the wave characterization using the simultaneous intensity and temperature data for July 2002 has remained largely untouched, these data are the subject of our study.

A summary of the observed temperature variability during July 2–19, 2002 is plotted in Fig. 1 as a contour of hourly averaged temperature data with day number along the x-axis. The data are averaged for 1 h to smooth out short-period waves, and this procedure enabled us to visualize and study the long-period structures in the data set. The temperature data exhibit large peak-to-peak variations of about 40 K during this period, with a range of 170 K to 210 K. The presence of periodic oscillations with periodicities of about 2 days in the data is interesting. This feature is evident in both the OH and O_2 temperature data. The phase of these features occurred during 0900–1300 UT near day

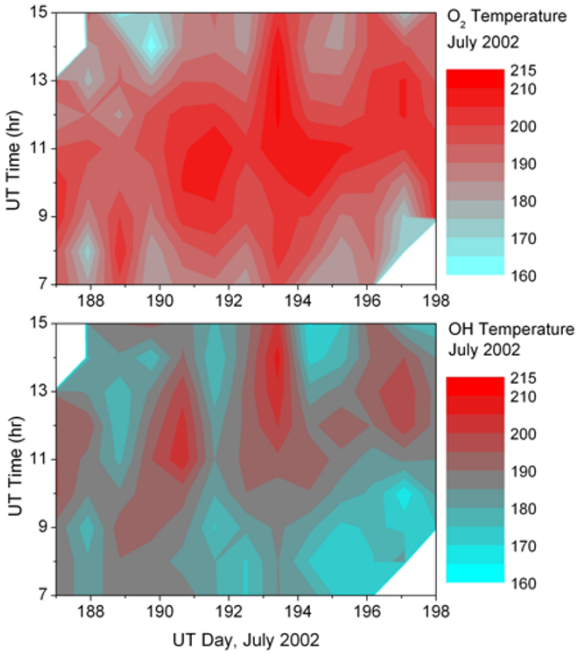

Fig. 1. A summary plot of mesospheric OH and O_2 temperature variations during July 2002 over Maui, Hawaii. Large night-to-night variability is evident in the plot.

numbers 189, 191, 193, and 195. A similar trend was evident in the intensity data. Without a detailed quantitative analysis, it is difficult to conclude whether this is a signature of the quasi 2-day wave in mesospheric temperatures, and limited night-time data restricted us from examining such possibilities. However, as the purpose of this plot is to summarize the temperature variability during July 2002, we refrain from discussions on the possibility of quasi 2-day wave and associated dynamics.

Further, as noted by Taori *et al.* (2005), the best-fit analysis on the variability of the nocturnal temperature exhibited an oscillation periodicity of 6–14 h, with large population of periodicity close to 8 h in the data set with amplitudes as large as 10–12 K. A Krassovsky analysis was carried out to better characterize this wave. As explained in Eq. (1), a Krassovsky analysis provides amplitude 'η' and phase 'φ' information, with amplitude being a measure of the effective transfer function of the density perturbation to cause the temperature perturbations and phase being a measure of the altitudinal difference between the corresponding fluctuations in their maxima in intensity and temperature profiles (Swenson and Gardner, 1998). Similar to the analysis described by Taori *et al.* (2005); a simple best-fit cosine model was used to determine the periodicity and amplitude of the perturbation in the nocturnal temperature and intensity data. An example of this analysis is shown in Fig. 2 for day number 190, 2002. A dominant long-period wave (principal wave) with short-period oscillatory features is evident in these data. The best-fit result shows that 8.6±0.1-h and 8.8±0.3-h waves with amplitude 10.5±0.4 K and 10.9±0.7 K are present in the OH and O_2 temperature data, respectively (small differences in values with earlier reported periodicities and amplitudes by Taori *et al.* (2005) are the result of different methods adopted for

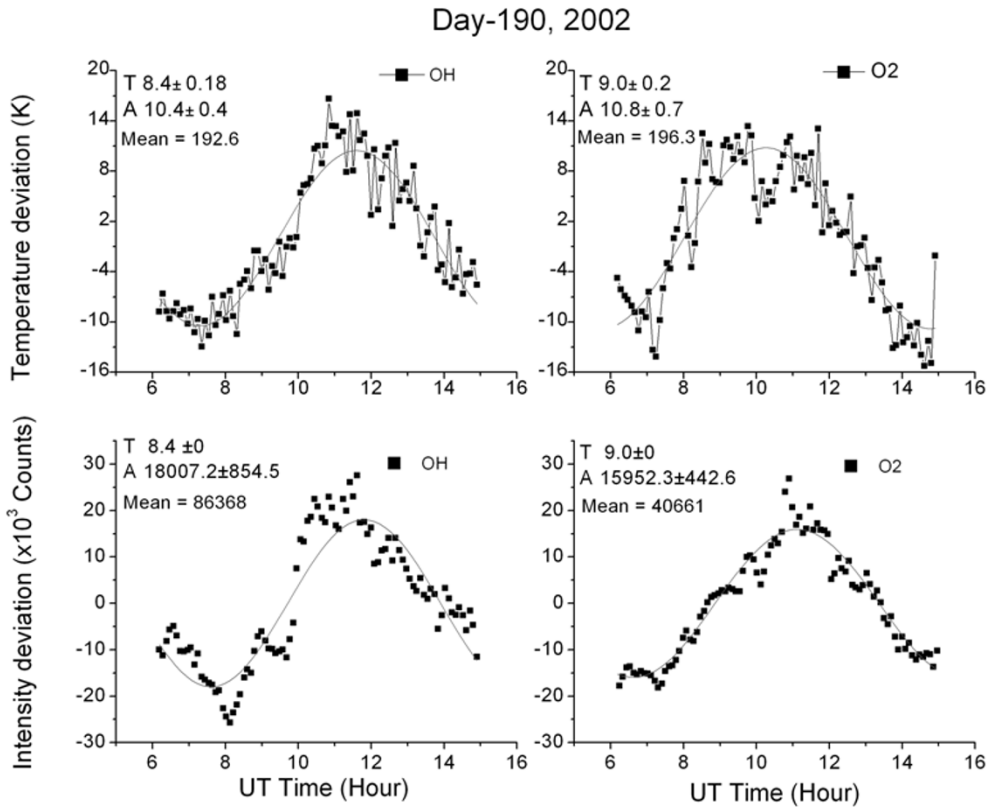

Fig. 2. An example of nocturnal variability in mesospheric OH and O_2 emissions. The connected symbols represent the mean deviations in OH and O_2 data for temperature (top panels) and intensity (bottom panels) variability for UT day 190, 2002. Solid lines in the plot show the result of a simple best-fit cosine model for an estimate on the principal wave periodicity and amplitude. Clearly visible in the data for both emissions is a long-period wave with a period of approximately 8 h.

Table 1. Derived wave parameters for OH data during July 2002.

Day no.	Wave period (h)	Relative temperature amplitude (%)	Relative intensity amplitude (%)	$\|\eta\|$	φ (degree)	λ_z (km)
183	6.3±1.0	3.2	5.6	1.72±0.97	−41.2±13.2	−116.6±72.6
187	7.2±0.4	3.5	11.1	3.13±0.68	−77±6.6	−43.3±9.5
188	7.6±0.2	4.9	16.0	3.24±0.34	−42.1±4.8	60.9±8.6
189	8.2±0.6	3.5	11.9	3.41±0.59	22.8±4.7	99.4±25.8
190	8.4±0.2	5.4	20.8	3.86±0.24	−14.57±4.3	−138±41.4
191	7.7±0.6	3.2	9.4	2.94±0.69	−27.58±5.1	−97.2±28.2
192	10.6±0.4	5.2	16.0	3.06±0.24	−25.5±8.5	−98.9±31.5
193	12.6±0.8	5.9	14.4	2.42±0.27	−26.57±3.3	−122.6±19.6
194	7.8±0.2	5.4	18.9	3.52±0.48	−26.1±4.5	−86.1±18.3
195	8.2±0.2	6.5	23.8	3.66±0.29	−13.17±4.4	−157.9±53.3
196	13.4±1.0	5.6	17.7	3.18±0.19	−16.08±2.9	−174.7±38
197	7.0±0.1	9.1	32.2	3.55±0.28	−52.45±5.2	−47±4.9
198	7.6±0.4	3.6	19.6	5.38±0.50	−41.21±5.2	−37.1±5.2
200	6.8±0.4	5.6	14.9	2.64±0.39	−90.53±7.4	−49.9±7.4

bad data point removal). The principal wave periodicities obtained from the temperature data are then forced to their corresponding intensity data for the best estimates of the amplitude and phase of the corresponding induced oscillations in intensities. The amplitude of Krassovsky's η has been calculated as given in Eq. (1). The nocturnal mean temperatures for OH and O_2 are 192.6 and 196.3 K, respectively, with mean band intensities (relative units/equivalent counts) of 86,368 (for OH) and 40,661 counts (for O_2), resulting in $|\eta|$ values of 3.86±0.24 and 7.13±0.50 for the OH and O_2 data, respectively. The phase values 'φ' of the Krassovsky parameter can be deduced by taking the difference between the intensity and temperature phase of the wave as described in Eq. (2). The intensity data for OH shows a lag of 0.25 h behind the temperature data, which is equivalent to an φ of approximately $-14.57\pm4.3^\circ$. Similarly, for the O_2 data, the intensity wave also lags behind the temperature one by approximately 0.4 h, giving rise to an φ of approximately $-33.6\pm4.0^\circ$. The above analysis was carried out on all 14 nights (Days 183–200), when prominent

Table 2. Derived wave parameters for O_2 data during July 2002.

Day no.	Wave period (h)	Relative temperature amplitude (%)	Relative intensity amplitude (%)	$\|\eta\|$	φ (degree)	λ_z (km)
183	8.5±2.0	9.4	45.2	4.79±0.80	−27.88±10.7	−59.6±23.6
187	7.5±0.8	5.7	31.5	5.53±0.95	−28.8±5.7	−49.8±12.4
188	10.2±0.8	4.6	25.8	5.65±0.91	−30.35±4.2	−46.2±9.5
189	8.2±0.6	6.5	28.3	4.33±0.61	−31.17±4.9	−59.2±11.9
190	9.0±0.2	5.5	39.2	7.13±0.50	−33.6±4.1	−33.7±4.3
191	8.8±0.5	5.2	30.5	5.91±1.07	−38.45±4.6	−35.9±7.5
192	9.0±0.3	5.5	27.1	4.90±0.39	−24±8.0	−76.5±29.1
193	9.8±0.4	2.9	38.3	12.88±1.01	−22.04±3.8	−27.6±5
194	8.1±0.2	5.7	48.3	8.40±0.39	−23.55±4.5	−39.3±7.3
195	8.3±0.2	5.9	38.0	6.37±0.32	−25.15±4.4	−48.6±8.2
196	11.4±0.4	3.2	31.8	9.94±0.71	−44.21±3.5	−19±1.8
197	8.2±0.1	8.6	71.8	8.29±0.37	−13.17±4.4	−69.8±23
198	6.9±0.2	3.5	20.5	5.91±0.56	−65.74±5.5	−24.5±2.6
200	7.6±0.2	5.6	48.2	8.59±0.47	−9.4±4.7	−96.3±49.3

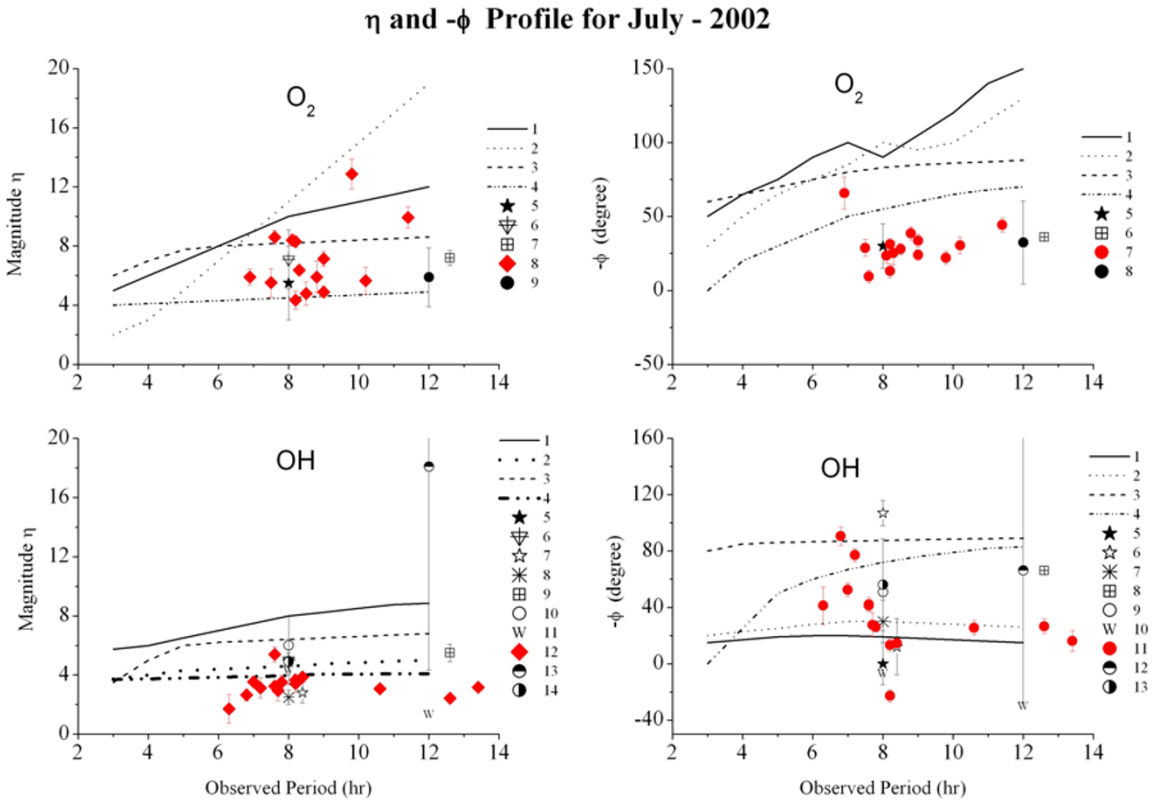

Fig. 3. A comparison of Krassovsky parameters for both OH and O_2 data to their respective wave periods. The x-axis shows the wave periodicity, and the y-axis is for Krassovsky parameters (η, φ) in each plot. A close resemblance between the observational values and discrepancy between the observational and theoretical estimates are noteworthy. The legends in the figure are as following: O_2 emission: (η: 1, Hickey *et al.* 500 km; 2, Hickey *et al.* 1000 km; 3, Tarasick and Shepherd 500 km; 4, Tarasick and Shepherd 1000 km; 5, Viereck and Deehr (1989); 6, Takahashi *et al.* (1992); 7, Reisin and Scheer (1996); 8, present study; 9, Lopez-Gonzalez *et al.* (2005)); (Φ: 1, Hickey *et al.* 500 km; 2, Hickey *et al.* 1000 km; 3, Tarasick and Shepherd, 500 km; 4, Tarasick and Shepherd, 1000 km; 5, Viereck and Deehr (1989); 6, Reisin and Scheer (1996); 7, present study; 8, Lopez-Gonzalez *et al.* (2005)). OH emission: ((η: 1, Schubert *et al.* 500 km; 2, Schubert *et al.* 1000 km; 3, Tarasick and Shepherd 500 km; 4, Tarasick and Shepherd 1000 km; 5, Viereck and Deehr (1989); 6, Takahashi *et al.* (1992); 7, Oznovich *et al.* (1995); 8, Drob *et al.* (1996); 9, Reisin and Scheer (1996); 10, Taylor *et al.* (2001); 11, Walterscheid and Schubert (1995); 12, present study; 13, Lopez-Gonzalez *et al.* (2005); 14, Oznovich *et al.* (1997)); (Φ: 1, Schubert *et al.* 500 km; 2, Schubert *et al.* 1000 km; 3, Tarasick and Shepherd 500 km; 4, Tarasick and Shepherd 1000 km; 5, Viereck and Deehr (1989); 6, Oznovich *et al.* (1995); 7, Drob *et al.* (1996); 8, Reisin and Scheer (1996); 9, Taylor *et al.* (2001); 10, Walterscheid and Schubert (1995); 11, present study; 12, Lopez-Gonzalez *et al.* (2005); 13, Oznovich *et al.* (1997)).

wave features were visible. It is noteworthy that during this period, the data is predominantly night waves with periods of approximately 8 h, with corresponding temperature amplitudes ranging from 5 to 15 K. Further, the $|\eta|$ values were found to vary from 1.7 to 5.4 for OH and from 4 to 12 for the O_2 data. The phase 'φ' values exhibit a larger variability, with values varying from -91° to $+23^\circ$. The vertical wavelength λ_z, calculated using $|\eta|$ and φ values with the

help of Eq. (3) turns out to be approximately -138 ± 41.4 and -33.7 ± 4.3 km for OH and O_2, respectively. Details of the deduced wave parameters are shown in Table 1 (for OH) and Table 2 (for O_2).

As mentioned above, the deduced Krassovsky parameters, show large differences from one night to other, indicating a high degree of dynamical variability at mesospheric altitudes during July 2002 over Hawaii. Figure 3 shows a comparison of our results for η and Φ with those of earlier reports, taking the average arithmetic value with respect to periodicity, which ranges from 6- to 12-h waves (Viereck and Deehr, 1989; Takahashi *et al*., 1992; Oznovich *et al*., 1995, 1997; Drob, 1996; Reisin and Scheer, 1996; Taylor *et al*., 2001; Lopez-Gonzalez *et al*., 2005), and model estimates of Schubert *et al*. (1991), Tarasick and Shepherd (1992a, b), Walterscheid and Schubert (1995), and Hickey *et al*. (1993). It is evident that the observed η and φ values in our study show a large spread in their distribution as compared to the model values. A similar spread in the distribution of observed values of $|\eta|$ has also been observed by other investigators (e.g., Takahashi *et al*., 1992). In the plot, error bars in our η and φ values represent the uncertainty in calculating the parameter, whereas in other investigators' cases, error bars are representative of the range of variability of deduced parameters in their respective reports. It is noteworthy that the values of η for the O_2 data in our study lie somewhere between the model estimates and the values observed by other investigators, whereas for OH, our η values are less than the model values on most occasions. The variation in the O_2 phase shows that most of the time we were observing values lower than the model estimates, whereas that for the OH phase fell between the ranges of model values of several authors.

In particular, Reisin and Scheer (1996) found mean values of $|\eta| = 5.5 \pm 0.6$ and $\varphi = -66^\circ$ for OH and of $|\eta| = 7.2 \pm 0.5$ and $\varphi = -36^\circ$ for O_2 for the simultaneous O_2 and OH observations. The deduced values with our OH and O_2 data compares well with those of Reisin and Scheer (1996), however, with the OH values being in approximate agreement. In another study, Lopez-Gonzalez *et al*. (2005), based on long-term observations with a spectral airglow temperature imager (SATI) from a mid-latitude station, reported a mean $|\eta|$ of approximately 5.89 for semi-diurnal tides during April to September for the O_2 data and an $|\eta|$ of approximately 18.1 for the OH data, with extreme variability (range shown in Fig. 3); these results do not agree with our results. In contrast, our observed $|\eta|$ (7.04 ± 0.65) is a good match with the O_2 emission values reported by Takahashi *et al*. (1992) (6.9 ± 0.3). In general, we find that there are significant differences in the calculated parameters for OH among various investigators. This may be due to the oxygen profile variability (Offermann *et al*., 1981) and $|\eta|$ dependence on O profile and complex OH chemistry (Walterscheid *et al*., 1994) at the OH altitude region. Another possible explanation may be the quenching of molecular lines by collision with perturbed molecules during the transitions from several vibrational levels, as discussed by Makhlouf *et al*. (1995), which can also affect the derived η parameter. At the same time, varying background wind conditions may also alter the deduced parameters (which should not be too different for OH and O_2 layers).

It is interesting to note that all the models show the phase φ for OH to be a negative value (or upward phase progression), with the exception of the model of Walterscheid and Schubert (1995). Our observed phases also show negative values (except for one night), corresponding with the values reported by other investigators. Our derived values for φ also closely match those based on other observations (Viereck and Deehr, 1989; Reisin and Scheer, 1996). However, one should note that modeled values show significant differences with observed ones. Differences in theory and observation may be due to the horizontal wavelength assumed in the model or the Prandtl number (ratio of kinematic viscosity to thermal diffusivity) assumed. The Prandtl number is important in theoretical calculations and modeling, especially when in terms of dissipating waves owing to molecular viscosity and thermal diffusivity while they propagate in the atmosphere. An error in the Prandtl number assumption will affect the derived wave parameters (λ_z, η etc.), which will in turn mask the actual ones.

The Doppler shifting of wave periods by the mean wind may also account for the discrepancy (Viereck and Deehr, 1989), creating a distinction between theoretical and observed periodicities. This distinction becomes relevant with the fact that during July 2002 mesospheric winds exhibited significant variability, as shown in figure 2 of Taori *et al*. (2005). Comparative studies between several investigators had also been discussed by Makhlouf *et al*. (1995) and Viereck and Deehr (1989). In particular, Makhlouf *et al*. (1995) attempted to account for the η characteristics by modifying Hine's model and using a new photochemical dynamical model (PDM); however, they were still unable to explain the appearance of the negative phases appropriately. Hines and Tarasick (1987) found a wide range of η variability, which is consistent with their theory, and Hines and Tarasick (1997) subsequently discussed the necessary correction for thin and thick layer approximations for the calculation of η from airglow emissions due to gravity waves interaction. Hines *et al*. (1997) pointed out that OH emission intensity, which affects the derived η, does not depend on the oxygen profile and other minor species; this contradicts the theory of Walterscheid *et al*. (1994), Schubert *et al*. (1991), and Offermann *et al*. (1981), as described in the previous section. In the light of above hypotheses, a large range in the observed η values are expected.

Observed vertical wavelength (VW) values for all the nights of the observation show significant differences between OH and O_2, as given in Fig. 4 where vertical bars indicate the error bar for our study and the ranges of variability for other investigators' studies plotted together. The VW for OH reveals a larger variability between $+99.44\pm3.8$ and -174.74 ± 16.5 km and that O_2 has a range of -19.06 ± 1.5 and -96.35 ± 5.9 km. The mean VW values for OH and O_2 are calculated to be -80.79 ± 15.4 and -49.02 ± 5.7 km, respectively, which are greater in magnitude than those of other investigators. Most of the days have negative values for φ and λ_z, indicating upward propagating gravity waves and tides—i.e., the downward phase progression. The values obtained by Reisin and Scheer (1996) and Lopez-Gonzalez *et al*. (2005) have also been shown in the plot

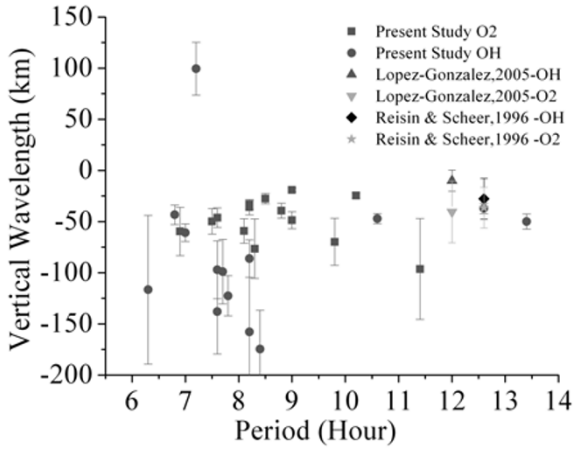

Fig. 4. Deduced vertical wavelengths (VW) for both the OH and O_2 emissions as a function of wave periodicity. Also shown are values obtained by other investigators for a comparison.

for a comparison. It is noteworthy that for all the days λ_{zOH} are generally higher than the λ_{zO_2}, which indicates the dissipation-dominated atmospheric conditions prevailing at that time, which reduce the vertical wavelength of the waves considerably as they propagate upward. Most probable contributing factors for such a dissipation are molecular viscosity and thermal diffusivity, with the latter acting as a filter of various periodicity waves at various altitudes (Hines, 1960). Vadas and Fritts (2005) have shown (equation (72) in their paper) that kinematic viscosity $\propto \lambda_z^3$, concluding that waves with a higher frequency and higher vertical wavelength will travel a higher altitude in a dissipation-dominated atmosphere and that this dissipating effect also increases with altitude, which is conspicuous in our results of decreasing λ_z with altitude. We have also found possible cases of evanescence (Tarasick and Hines, 1990) for OH where $\lambda_{zOH} \geq 100$ km. A few cases of evanescence were also found by Reisin and Scheer (1996). Our values lie well within the ranges reported by other investigators. Noteworthy, the values reported by Reisin and Scheer (1996), who found a mean VW for OH of approximately -30 km and one for O_2 of approximately -40 km, with $\sim$40 km variability, are somewhat in agreement with our values. However, Lopez-Gonzalez *et al*. (2005) observed approximately the same values—around approximately -10 km for OH and approximately -40 km for molecular oxygen.

Overall, although there has been significant progress made in our understanding of the effects of gravity waves on airglow emissions with the use of Krassovsky analysis, very little data are available on ter-diurnal type of waves. Given that our data sets focus on the 8-h periodicity wave, our results are important. The aim of our study is to fill the gaps of Krassovsky parameters between the semi-diurnal range and short period (0.5–1 h) waves. The observed variability in our data surely indicates conspicuous signatures of wave activities in the mesopause region. Interestingly, a comparison with other observations and model values exhibit no systematic agreement, thereby illustrating the necessity for more detailed data with supplementary imagery and wind information.

Acknowledgments. The present analysis work is supported by ARIES (DST, Govt. of India) and NARL (DOS, Govt. of India). The observations were conducted as a part of an ongoing joint program between National Science Foundation (NSF) and Air Force Office of Scientific Research (AFOSR). Financial support for the measurements was provided by NSF grant ATM 0003218. A. Taori was supported as a CEDAR Post Doctoral Fellow under NSF Grant ATM 0134150.

References

Drob, D. P., Ground-based optical detection of atmospheric waves in the upper mesosphere and lower thermosphere, Ph. D. Thesis, University of Michigan, Ann Arbor, MI, 1996.

Fritts, D. C. and M. J. Alexander, Gravity wave dynamics and effects in the middle atmosphere, *Rev. Geophys*., **41**(1), 1003, doi: 10.1029/2001RG000106, 2003.

Gardner, C. S. and M. J. Taylor, Observational limits for lidar, radar, and airglow imager measurements of gravity wave parameters, *J. Geophys. Res*., **103**, 6427–6437, 1998.

Hickey, M. P., G. Schubert, and R. L. Walterscheid, Gravity wave driven fluctuations in the O_2 atmospheric (0–1) nightglow from an extended, dissipative emission region, *J. Geophys. Res*., **98**, 13,717–13,729, 1993.

Hines, C. O., Internal atmospheric gravity waves at ionospheric heights, *Can. J. Phys*., **38**, 1441–1481, 1960.

Hines, C. O., A fundamental theorem of airglow fluctuations induced by gravity waves, *J. Atmos. Sol. Terr. Phys*., **59**, 319–326, 1997.

Hines, C. O. and D. W. Tarasick, On the detection and utilization of gravity waves in airglow studies, *Planet. Space Sci*., **35**, 851–866, 1987.

Hines, C. O. and D. W. Tarasick, Layer truncation and the Eulerian/ Lagrangian duality in the theory of airglow fluctuations induced by gravity waves, *J. Atmos. Sol. Terr. Phys*., **59**, 327–334, 1997.

Krassovsky, V. I., Infrasonic variation of OH emission in the upper atmosphere, *Ann. Geophys*., **28**, 739–746, 1972.

Lopez-Gonzalez, M. J. *et al*., Tidal variations of O_2 Atmospheric and OH(6-2) airglow and temperature at mid-latitude from SATI observations, *Ann. Geophys*., **23**, 3579–3590, 2005.

Makhlouf, U. B., R. H. Picard, and J. R. Winick, Photochemical-dynamical modeling of the measured response of airglow to gravity waves, 1: basic model for OH airglow, *J. Geophys. Res*., **100**, 11,289–11,311, 1995.

Murthy, B. V. K., Middle atmosphere-upper atmosphere coupling, *Proc. Ind. Natl. Sci. Acad*., **64**, A, 3, 303–313, 1998.

Offermann, D., V. Friedrich, P. Ross, and U. von Zahn, Neutral gas composition measurements between 80 and 120 km, *Planet. Space Sci*., **29**, 747–764, 1981.

Oznovich, I., D. J. McEwen, and G. G. Sivjee, Temperature and airglow brightness oscillations in the polar mesosphere and lower thermosphere, *Planet. Space Sci*., **43**, 1121–1130, 1995.

Oznovich, I., R. L. Walterscheid, G. G. Sivjee, and D. J. McEwen, On Krassovsky's ratio for ter-diurnal hydroxyl oscillations in the winter polar mesopause, *Planet. Space Sci*., **45**(3), 385–394, 1997.

Pancheva, D. V., P. J. Mukhtarov, M. G. Shepherd, N. J. Mitchell, D. C. Fritts, D. M. Riggin, S. J. Franke, P. P. Batista, M. A. Abdu, I. S. Batista, B. R. Clemesha, and T. Kikuchi, Two-day wave coupling of the low-latitude atmosphere-ionosphere system, *J. Geophys. Res*., **111**, A07313, doi:10.1029/2005JA011562, 2006.

Reisin, E. R. and J. Scheer, Characteristics of atmospheric waves in the tidal period range derived from zenith observations of O_2 (0-1) Atmospheric and OH (6-2) airglow at lower midlatitudes, *J. Geophys. Res*., **101**, 21,223–21,232, 1996.

Schubert, G., R. L. Walterscheid, and M. P. Hickey, Gravity wave-driven fluctuations in OH nightglow from an extended, dissipative emission region, *J. Geophys. Res*., **96**(A8), 13,869–13,880, 1991.

Suzuki, S., K. Shiokawa, Y. Otsuka, T. Ogawa, K. Nakamura, and T. Nakamura, A concentric gravity wave structure in the mesospheric airglow images, *J. Geophys. Res*., **112**, D02102, doi:10.1029/2005JD006558, 2007.

Swenson, G. R. and C. S. Gardner, Analytical model for the response of the mesosphere OH* and Na layers to atmospheric gravity waves, *J. Geophys. Res*., **103**, 6271–6294, 1998.

Takahashi, H., Y. Sahai, P. P. Batista, and B. R. Clemesha, Atmospheric gravity wave effect on the airglow O_2 (0-1) and OH (9-4) band intensity and temperature variations observed from a low latitude station, *Adv. Space Res*., **12**(10), 131–134, 1992.

Takahashi, H., P. P. Batista, R. A. Buriti, D. Gobbi, T. Nakamura, T. Tsuda,

and S. Fukao, Response of the airglow OH emission, temperature and mesopause wind to the atmospheric wave propagation over Shigaraki, Japan, *Earth Planets Space*, **51**, 863–875, 1999.

Takahashi, H., R. A. Buriti, D. Gobbi, and P. P. Batista, Equatorial planetary wave signatures observed in mesospheric airglow emissions, *J. Atmos. Solar. Terr. Phys.*, **64**, 1263–1272, 2002.

Taori, A. and M. Taylor, Characteristics of wave induced oscillations in mesospheric O_2 emission intensity and temperatures, *Geophys. Res. Lett.*, **33**, L01813, doi:10.1029/2005GL024442, 2006.

Taori, A., M. J. Taylor, and S. Franke, Terdiurnal wave signatures in the upper mesospheric temperature and their association with the wind fields at low latitudes (20°N), *J. Geophys. Res.*, **110**, D09S06, doi:10.1029/2004JD004564, 2005.

Taori, A., A. Guharay, and M. J. Taylor, On the use of simultaneous measurements of OH and O_2 emissions to investigate wave growth and dissipation, *Ann. Geophys.*, **25**, 639–643, 2007.

Tarasick, D. W. and C. O. Hines, The observable effects of gravity waves in airglow emission, *Planet. Space Sci.*, **38**, 1105–1119, 1990.

Tarasick, D. W. and G. G. Shepherd, Effects of gravity waves on complex airglow chemistries: 1. O_2 ($b^1\Sigma_g^+$) emission, *J. Geophys. Res.*, **97**, 3185–3193, 1992a.

Tarasick, D. W. and G. G. Shepherd, Effects of gravity waves on complex airglow chemistries: 2. OH emission, *J. Geophys. Res.*, **97**, 3195–3208, 1992b.

Taylor, M. J., L. C. Gardner, and W. R. Pendleton, Jr., Long-period wave signatures in mesospheric OH Meinel (6,2) band intensity and rotational temperature at mid-latitudes, *Adv. Space Res.*, **27**(6–7), 1171–1179, 2001.

Vadas, S. L. and D. C. Fritts, Thermospheric responses to gravity waves: Influences of increasing viscosity and thermal diffusivity, *J. Geophys. Res.*, **110**, D15103, doi:10.1029/2004JD005574, 2005.

Viereck, R. A. and C. S. Deehr, On the interaction between gravity waves and the OH Meinel (6-2) and O_2 Atmospheric (0-1) bands in the polar night airglow, *J. Geophys. Res.*, **94**, 5397–5404, 1989.

Vincent, R. A. and D. Lesicar, Dynamics of the equatorial mesosphere: First results with a new generation partial reflection radar, *Geophys. Res. Lett.*, **18**, 825–828, 1991.

Walterscheid, R. L. and G. Schubert, Dynamical-chemical model of fluctuations in the OH airglow driven by migrating tides, stationary tides, and planetary waves, *J. Geophys. Res.*, **100**, 17,443–17,449, 1995.

Walterscheid, R. L., G. Schubert, and M. P. Hickey, Comparison of theories for gravity wave fluctuations in airglow emissions, *J. Geophys. Res.*, **99**, 3935–3944, 1994.

A. Guharay, A. Taori (e-mail: taori@narl.gov.in), and M. Taylor